Intratumoral heterogeneity of receptor tyrosine kinases EGFR and PDGFRA amplification in glioblastoma defines subpopulations with distinct growth factor response

Nicholas J. Szerlip[a], Alicia Pedraza[b], Debyani Chakravarty[b], Mohammad Azim[c], Jeremy McGuire[c], Yuqiang Fang[d], Tatsuya Ozawa[e], Eric C. Holland[e,f,g,h], Jason T. Huse[d,h], Suresh Jhanwar[d], Margaret A. Leversha[c], Tom Mikkelsen[i], and Cameron W. Brennan[b,f,h,1]

[a]Department of Neurosurgery, Wayne State University Medical School, Detroit, MI 48201; [b]Human Oncology and Pathogenesis Program, [c]Molecular Cytogenetic Core Laboratory, [d]Department of Pathology, [e]Cancer Biology and Genetics Program, [f]Department of Neurosurgery, [g]Department of Surgery, and [h]Brain Tumor Center, Memorial Sloan-Kettering Cancer Center, New York, NY 10065; and [i]Departments of Neurology and Neurosurgery, Henry Ford Health System, Detroit, MI 48202

Edited by Webster K. Cavenee, Ludwig Institute, University of California at San Diego, La Jolla, CA, and approved December 29, 2011 (received for review August 29, 2011)

Glioblastoma (GBM) is distinguished by a high degree of intratumoral heterogeneity, which extends to the pattern of expression and amplification of *receptor tyrosine kinases* (RTKs). Although most GBMs harbor RTK amplifications, clinical trials of small-molecule inhibitors targeting individual RTKs have been disappointing to date. Activation of multiple RTKs within individual GBMs provides a theoretical mechanism of resistance; however, the spectrum of functional RTK dependence among tumor cell subpopulations in actual tumors is unknown. We investigated the pattern of heterogeneity of RTK amplification and functional RTK dependence in GBM tumor cell subpopulations. Analysis of The Cancer Genome Atlas GBM dataset identified 34 of 463 cases showing independent focal amplification of two or more RTKs, most commonly platelet-derived growth factor receptor α (PDGFRA) and epidermal growth factor receptor (EGFR). Dual-color fluorescence in situ hybridization was performed on eight samples with *EGFR* and *PDGFRA* amplification, revealing distinct tumor cell subpopulations amplified for only one RTK; in all cases these predominated over cells amplified for both. Cell lines derived from coamplified tumors exhibited genotype selection under RTK-targeted ligand stimulation or pharmacologic inhibition in vitro. Simultaneous inhibition of both EGFR and PDGFR was necessary for abrogation of PI3 kinase pathway activity in the mixed population. DNA sequencing of isolated subpopulations establishes a common clonal origin consistent with late or ongoing divergence of RTK genotype. This phenomenon is especially common among tumors with *PDGFRA* amplification: overall, 43% of *PDGFRA*-amplified GBM were found to have amplification of *EGFR* or the hepatocyte growth factor receptor gene (*MET*) as well.

glioma | glioblastoma genetics | mosaicism | amplicon

Glioblastoma (GBM) is the most common primary malignant brain tumor in adults and is characterized by histologic intratumoral heterogeneity, invasive growth patterns, and overall poor response to treatment with conventional radiation and chemotherapy (1, 2). The majority of primary GBMs harbor amplification and/or mutation of a receptor tyrosine kinase (RTK): either epidermal growth factor receptor (*EGFR*; 40–50%), platelet-derived growth factor receptor α (*PDGFRA*; ≈15%), or the hepatocyte growth factor receptor (*MET*, ≈5%) (3, 4). The high prevalence of *EGFR* and *PDGFRA* alterations seen in GBM has nominated these RTKs as priority candidates for therapeutic targeting. However, clinical trials of small-molecule inhibitors targeting EGFR and PDGFR used as single therapy have shown little response in unselected patients, and amplification status of the receptors has not yet been found to be predictive (5–10).

One hypothesis for the therapeutic failure of targeting a single RTK in GBM even when the gene is amplified or mutated is that other RTKs may be concurrently activated in the same tumor. In fact, concurrent phosphorylation of multiple RTKs has been demonstrated in GBM and has been shown to mediate resistance to single-RTK inhibition through "RTK switching" in cell lines (11). Although such RTK coactivation has been measured at the protein level, its significance in maintaining tumor cell subpopulations has not been established.

We have previously reported prominent PDGFR activation by platelet-derived growth factor beta (PDGFB) ligand in GBMs with *EGFR* or *MET* amplification (12). We hypothesized that this could lead to cases wherein *PDGFRA* is amplified along with either *EGFR* or *MET* in the same tumor, signifying that both RTKs contribute to positive growth advantage. Amplifications of *EGFR* and *PDGFRA* are often heterogeneously distributed in GBM, and retention of the amplicons is thought to depend on positive selection pressure (13, 14). Finding cases of GBM with focal amplification of two or more RTKs affords an opportunity to identify by FISH whether this positive selection favors amplification of both receptors in the same cells or in different populations and, if the populations are distinct, whether they are regionally segregated in the tumor.

In this study we establish the prevalence of RTK coamplification from analysis of data from The Cancer Genome Atlas (TCGA) pilot project, examine the anatomic/cellular relationship of *EGFR* and *PDGFRA* amplifications in select cases by FISH, and investigate the phenomenon of in vitro selection of *EGFR*- and *PDGFRA*-amplified genotypes from genetically heterogeneous cell lines derived from coamplified tumors.

Results

Common Focal RTK Amplifications in GBM Are Not Mutually Exclusive and Define Subpopulations. From the TCGA dataset, array comparative genomic hybridization (aCGH) profiles of 463 GBMs were examined for focal copy number aberration (CNA) spanning *EGFR*, *PDGFRA*, or *MET*. CNA focality was determined by a previously described algorithm, genome topography scan (GTS, available as R package from http://cbio.mskcc.org/brennan; *SI Methods*) (15). Amplifications or gains were scored for RTKs commonly altered in GBM: *EGFR*, *MET*, and the region of chr4q12 spanning three neighboring RTKs *PDGFRA*, *KIT*, and *KDR* ("*PDGFRA*-region"). GTS focality scores above 0.02,

Author contributions: N.J.S., A.P., D.C., E.C.H., and C.W.B. designed research; N.J.S., A.P., D.C., M.A., J.M., Y.F., T.O., J.T.H., M.A.L., and C.W.B. performed research; T.O., S.J., M.A.L., T.M., and C.W.B. contributed new reagents/analytic tools; N.J.S., A.P., D.C., E.C.H., J.T.H., S.J., and C.W.B. analyzed data; and N.J.S. and C.W.B. wrote the paper.

The authors declare no conflict of interest.

This article is a PNAS Direct Submission.

Freely available online through the PNAS open access option.

[1]To whom correspondence should be addressed. E-mail: cbrennan@mskcc.org.

This article contains supporting information online at www.pnas.org/lookup/suppl/doi:10.1073/pnas.1114033109/-/DCSupplemental.

implying CNA shared with 50 or fewer neighboring genes, were considered candidate focal amplifications. Of 463 GBM profiles examined, focal *PDGFRA*-region amplification was found in 74 (16%). In many of these cases, *PDGFRA* was either the only RTK in the amplicon or was the only RTK spanned by the peak of the CNA (n = 29, 39%). In contrast, *KIT* and *KDR* were never independently amplified. Most cases showed amplification equally across *PDGFRA* and *KIT* (n = 17) or *PDGFRA*, *KIT*, and *KDR* (n = 28). Because *PDGFRA* is the only RTK consistently amplified in the locus and is a known target of mutation in GBM (16), we refer to *PDGFRA*-region amplification simply as *PDGFRA* amplification. Focal amplification of *EGFR* was found in 214 samples (46%) and of *MET* in 12 samples (2.6%).

Coamplifications of *EGFR*, *MET*, and/or *PDGFRA* were observed in 34 samples (7.3% of TCGA GBM). Remarkably, 43% of *PDGFRA*-amplified tumors demonstrated coamplification of either *EGFR* or *MET*. Of the 12 *MET*-amplified tumors, 3 had *EGFR* and 5 had *PDGFRA* amplification (including one case with both). Fig. 1*A* summarizes the incidence of focal CNA found among the three RTKs considered. Focal CNA involving *PDGFRA* and/or *EGFR* typically reached log2 ratios above 2, implying an average of more than eight gene copies per cell (Fig. 1*B*).

In many coamplified cases the locus log2 ratios were below 2 and in the range commonly associated with gains of broad chromosomal regions or chromosomal arms. However, the high GTS focality scores rule out broad CNA and suggest instead that focal high-level amplifications in a subpopulation of tumors cells are being diluted by unamplified cells. To investigate this further, formalin-fixed, paraffin-embedded (FFPE) tissue specimens were identified at the Hermelin Brain Tumor Center at Henry Ford Cancer Center for six tumors in the TCGA set with focal *EGFR* and *PDGFRA* CNA (aCGH profiles of the matching TCGA samples are shown in Fig. S1*A*).

FISH probes for *PDGFRA*, *EGFR*, and chr7 centromeric region (CEN7) were validated on frozen and FFPE samples and used to examine the distribution of amplified cells. In addition to six samples from the TCGA case series, 2 out of 120 tumors from the Memorial Sloan-Kettering Cancer Center (MSKCC) Brain Tumor Center tissue bank were identified harboring coamplification for *EGFR* and *PDGFRA* (aCGH shown in Fig. S1*B*). Slides were reviewed by the MSKCC Clinical Cytogenetics Laboratory for routine scoring of the percentage of cells harboring high-level amplification (eight or more copies) of either *EGFR* or *PDGFRA* out of 200 tumor cells per random high-power field. In all eight cases examined, FISH confirmed that focal CNA, regardless of amplitude, signified high-level RTK amplification in a subpopulation of cells. Overall, *EGFR* amplification was seen in 40–70% of cells and *PDGFRA* amplification in 10–30% (Fig. 2). In all cases examined, the pattern of amplification appeared to be either exclusively or predominantly of extrachromosomal double minute form.

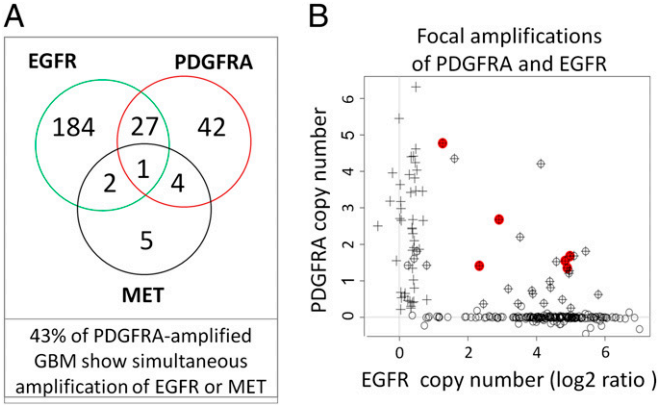

Fig. 1. RTKs such as *EGFR* and *PDGFRA* are targets of focal amplification in GBM and can both be amplified in the same tumor. (*A*) Venn diagram depicting the incidence of individual RTK amplifications and the cooccurrence of two or more RTKs amplified in the same tumor. (*B*) aCGH data from 463 cases of primary GBM from TCGA were analyzed by GTS to identify focal CNA spanning *EGFR* and/or *PDGFRA*. For 241 cases showing focal events, mean log2 ratio is plotted for *EGFR* ("O") and *PDGFRA* ("+"). Thirty-four tumors show focal CNA at both RTKs. Red denotes cases selected for FISH investigation.

EGFR and *PDGFRA* amplification was then assessed by dual-color FISH to determine the overlap in distribution. As shown in Fig. 2, all tumors demonstrated a common pattern in which the majority of cells showed amplification of a single RTK (either *EGFR* or *PDGFRA*). The fraction of cells harboring amplification of both receptors ranged from 0 to 28% but comprised a minority of the population in all cases. Examples of dual-color FISH are shown in Fig. 3. *PDGFRA*-amplified and *PDGFRA*/*EGFR*-coamplified cells were typically broadly distributed throughout the tumors and were in all cases interspersed with *EGFR*-amplified and nonamplified cells (example in Fig. S2). All tumors demonstrated regions without *PDGFRA*-amplified cells (i.e., *EGFR*-amplified only) but the converse, a region with exclusive *PDGFRA*-amplified cells, was not seen in any sample.

Genomic Characteristics of RTK-Coamplified Tumors. Analysis of TCGA genomic data found no distinguishing characteristics of dual RTK coamplified tumors compared with other GBMs. There were no differences in patient age (57.87 vs. 57.67 y) or survival (median 318 d vs. 427 d, P = 0.1, Cox proportional hazards). Furthermore, comparison of coamplified GBMs to single RTK-amplified tumors found equivalent overall rates of autosomal CNA, a measure of genomic instability (88.4 vs. 87.3, P = 0.9, Student t test). Similarly, excluding seven hypermutated cases (none of which were coamplified), the overall incidence of mutation was no different among 698 genes for which TCGA data are currently available.

A single *EGFR* extracellular domain point mutation was noted among the 11 coamplified cases for which sequencing data were available (TCGA-06-0616, G598V). Status of the most common activating *EGFR* mutation, *EGFRvIII* deletion, is not reported for TCGA specimens but may be inferred in some cases by evidence of genomic deletion on aCGH (*Methods*). Of the 61 of 463 cases for which relative deletion between introns 1 and 7 can be discerned, 50 have focal *EGFR* amplification, and 11 of these have coamplification of *PDGFRA*. Therefore, there was a trend for higher prevalence of *EGFRvIII* mutation among *EGFR* coamplified cases (36.7%, 11 of 30) compared with tumors with sole *EGFR* amplification (21%, 39 of 184), although this did not reach significance (Fisher exact test, P = 0.1). A single case of *PDGFRA* point mutation was reported among the coamplified tumors (TCGA-06-0174, W349C) although the functional significance is unknown. The most common form of *PDGFRA* activating mutation in GBM is the $PDGFRA^{\Delta 8,9}$ deletion (16). This narrow deletion could not be assessed in the TCGA dataset because of inadequate coverage by microarrays. For the two coamplified cases for which frozen tissue was available (M561 and M753), RT-PCR assays for *EGFRvIII* and $PDGFRA^{\Delta 8,9}$ found no evidence of either mutation. Similarly, gene resequencing identified no extracellular domain or kinase-domain point mutations in either *EGFR* or *PDGFRA* in these two samples.

Four transcriptomal subclasses of primary GBM have been reported by TCGA, and these differ somewhat in the prevalence of RTK alterations: the *Classical* subclass is enriched for *EGFR* amplifications (95%); the *Proneural* subclass is associated with *PDGFRA* amplification (35%), and nearly all GBM with *MET* amplification belong in this subclass; the *Neural* subclass shows a diversity of RTK amplification without enrichment for any particular genotype; the *Mesenchymal* subclass shows *EGFR* amplifications (29%) and rarely *PDGFRA* (9%) (17). In accordance with the larger TCGA sample set, the coamplified cases appear transcriptomally diverse (Fig. S3). There was a tendency for the coamplified specimens to belong to Proneural, Classical,

		200 tumor cells per random HPF		200 tumor cells with either amplification		
Sample	TCGA ID	Total EGFR amp.	Total PDGFRA amp.	EGFR amplified only	EGFR + PDGFRA dual-amplified	PDGFRA amplified only
T143	TCGA-06-0143	57%	21%	61%	1.5%	38%
T214	TCGA-06-0214	40%	15%	20%	28%	52%
T211	TCGA-06-0211	66%	13%	60%	20%	20%
T174	TCGA-06-0174	58%	27%	60%	5%	35%
T402	TCGA-06-0402	71%	16%	81%	2%	17%
T155	TCGA-06-0155	50%	9%	69%	2.5%	29%
M561	--	60%	28%	70%	0%	30%
M753	--	56%	25%	64%	8%	28%

Fig. 2. Summary of single and multicolor FISH results for *EGFR* and *PDGFRA* in eight GBM with aCGH evidence of amplification at both loci. *EGFR* and *PDGFRA* amplification was defined as more than eight copies per cell and was first scored for each locus individually in 200 cells of a random high-power field (HPF) by single-color FISH (*Left*). Amplicon colocalization was evaluated by dual-color FISH in 200 cells that harbored one or more amplification events (*Right*). In all cases studied, *EGFR* and *PDGFRA* amplification was found predominantly in distinct tumor cell subpopulations. Overall, *EGFR* amplification was more prevalent than *PDGFRA* amplification.

and Neural classes more than Mesenchymal, although this may reflect the relative paucity of RTK amplification in the Mesenchymal class overall. Interestingly, among samples with both *EGFR* and *PDGFRA* amplification, those closer to the Proneural centroid had higher PDGFRA log2 ratios (3.03 vs. 1.13, $P = 0.0300$), and those closer to the Classical centroid had higher EGFR ratios (4.32 vs. 1.48, $P = 0.0029$), suggesting that the transcriptomal signature may be driven in part by the balance of genomic and signaling alterations.

EGFR- and PDGFRA-Amplified Subpopulations Are Dynamic Under in Vitro Growth Conditions. For tumors M561 and M753, tumor sphere lines were reexpanded from early-passage tumor sphere cultures that had initially been isolated in neural stem cell media with EGF/FGF supplement and cryogenically banked. After reexpansion, both tumor sphere lines demonstrated maintenance of genetic heterogeneity at early passages. However, exogenous growth factors in the media altered the population distributions of the cells over time.

In M561-derived cells, both *EGFR* and *PDGFRA* amplifications were present by aCGH at mean levels comparable to the initial tumor after ≈4 wk in culture. However, prolonged growth in neural stem cell media with FGF and either EGF, PDGFB, or EGF+PDGFB supplement led to loss of both focal amplifications. For the tumor sphere line derived from M753 (TS753), early passage in neural stem cell media with EGF+FGF supplement yielded a heterogeneous population of cells, all of which harbored *EGFR* amplification and 20% showing *PDGFRA* amplification as well. Although *PDGFRA*/*EGFR*-coamplified cells were relatively rare in the original tumor (8%), they were a significant and stable cell fraction of 20–30% in long-term cultures assessed periodically by FISH (Fig. S4). Protein expression of EGFR and PDGFRA assessed by FACS revealed an expected bimodal distribution of PDGFRA expression and ubiquitous EGFR expression, concordant with genotype (Fig. S5*A*).

The TS753 line was used to investigate whether specific amplified subpopulations emerge during serial expansion in three different conditions of growth factor supplement: EGF ligand only, EGF and PDGFB, and PDGFB only. Cultures were expanded for 13 wk and FISH performed at 4-wk intervals. Cells with more than six signals were classified as amplified. Under PDGFB ligand supplementation, the percentage of *PDGFRA*/*EGFR*-coamplified cells increased from 26% initially to 54% after 4 wk and to 79% at 8 wk (Fig. S4). Cells grown in EGF supplement over the same period demonstrated relative stability of genotype, with persistence of *PDGFRA*/*EGFR* coamplified fraction at ≈25%. EGF+PDGFB supplementation had an intermediate effect, with partial expansion of the *PDGFRA*/*EGFR* coamplified fraction to 30% at 4 wk and to 34% at 8 wk (Fig. S4).

Although PDGFB ligand selected for cells with *PDGFRA*-amplified genotype, the overall number of *EGFR* signals per cell in the coamplified cells diminished over time. In the initial cell population all cells demonstrated high levels of amplifications (>20 signals). After 8 wk growth in PDGFB a significant portion of *PDGFRA*/*EGFR* coamplified cells (30%) had lower levels of *EGFR* amplification (3–12 copies per cell). After 13 wk *EGFR* copy number fell below six copies in most cells (Fig. S4*B*). In comparison, cells grown with EGF ligand demonstrated persistent high levels of *EGFR* amplification in all cells at 13 wk and high levels of *PDGFRA* amplification in a coamplified fraction that expanded to 31% from 26% initially.

The persistence and expansion of *PDGFRA*/*EGFR* coamplified cells under EGF stimulation suggests some growth advantage conferred by high expression of PDGFR (the only RTK in the locus) despite an absence of explicit stimulation by external PDGFB ligand. Therefore, after 8 wk of in vitro passage in EGF, the PDGFRA inhibitor imatinib (5 μM) was added and cells passaged for an additional 4 wk. Imatinib led to substantial loss of the *PDGFRA*/*EGFR* coamplified cells at 12 wk (11%) compared with uninhibited cells (31%). Similarly, addition of 0.5 μM gefitinib (an EGFR inhibitor) to the PDGFB supplement led to further selection of *PDGFRA*/*EGFR* coamplified cells (86% from 80%).

TS753 cells of mixed genotype (25% *PDGFRA*-amplified, 100% *EGFR*-amplified) demonstrated no constitutive phosphorylation of either RTK, consistent with their wild-type genotypes, as determined by resequencing and by RT-PCR for the common deletion mutations *EGFRvIII* and *PDGFRA*[4,8,9]. Further, under dual-ligand stimulation, the addition of 4 μM gefitinib or 10 μM imatinib inhibited their respective targets, as demonstrated by a decrease in phosphorylation of EGFR and PDGFRA, respectively (Fig. S6*A*). The activation states of the PI3-kinase and mTOR pathways, as measured by phosphorylation of AKT and S6-kinase, were mildly decreased with single

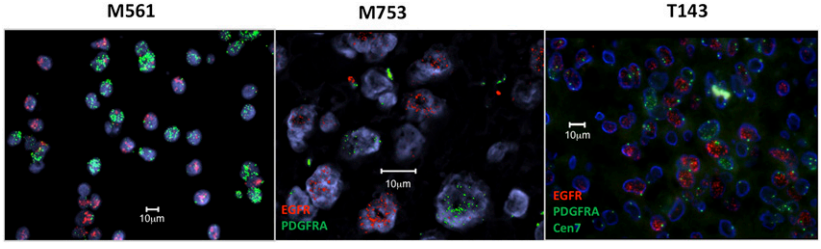

Fig. 3. FISH reveals distinct tumor cell subpopulations with *EGFR* or *PDGFRA* amplification. Dual-color FISH of a touch prep of frozen tumor M561 (*Left*), FFPE sample M753 (*Center*), and FFPE of T143 (*Right*) demonstrate *EGFR* and *PDGFRA* amplification to be distributed nonuniformly and to define independent populations with distinct RTK genotypes. For M561, green and red probes mark *EGFR* and *PDGFRA*, respectively. For M753, green and red denote *PDGFRA* and *EGFR*, respectively. For T143, green denote two separate probes for *PDGFRA* and centromere 7 and red denotes *EGFR*. (Original magnification: 40×; scale bars, 10 μm.)

inhibition of either RTK and more strongly attenuated with combined inhibition.

Interestingly, gefitinib led to dephosphorylation of PDGFRA sites Y720, Y849, and Y742 at concentrations as low as 0.5 μM (Fig. S6*B*). Binding partners for two of these sites, SHP-2 (Y720) and PI3K (Y742), have recently been shown to contribute significantly to glioma tumorigenesis in PDGFRA-driven, Ink4a/ARF-deficient gliomas; tumorigenicity was abrogated by mutation of either tyrosine site or by pharmacologic inhibition of SHP-2 or PI3K (18). In the TS753 line, we found that dephosphorylation of Y720 and Y742 by gefitinib was associated with loss of Erk phosphorylation, whereas p-Akt and p-S6K remained elevated and responsive to addition of imatinib (Fig. S6*A*). We investigated this phenomenon in a second tumor sphere line, TS543, which harbors amplification of PDGFRA and expresses high levels of $PDGFRA^{\Delta 8,9}$ but very low levels of EGFR (as measured by Western blot). Gefitinib treatment (4 μM) led to loss of PDGFRA phosphorylation at sites Y720 and Y842 but not of Y742 (Fig. S6*C*). As with TS753, Akt phosphorylation in TS543 remained high, whereas imatinib has been shown to inhibit p-Akt in this line (16). We conclude that the effects of gefitinib on PDGFRA tyrosine phosphorylation sites are not restricted to EGFR/PDGFRA coamplified cells and can occur in the context of very low EGFR expression levels. In our experiments, gefitinib does not abolish imatinib-sensitive Akt activation when PDGFRA is activated by ligand or mutation. These results suggest the possibility of significant direct interactions between EGFR and PDGFRA in coamplified cells, but they also indicate a component of PDGFRA signaling that may require specific targeting, separately from EGFR.

Divergence of Multiple RTK-Amplified Cell Populations Is a Late Event in Tumor Evolution. We next investigated whether distinct RTK-amplified subpopulations represent independent clonal tumor expansions or divergent populations from a common clonal origin. Allelic frequencies of mutations in the M753 parent tumor were compared with frequencies in the TS753 lines expanded under PDGFB vs. EGF ligand, which provided skewed populations in which either 80% or 27% of the cells were *PDGFRA*/*EGFR* coamplified, respectively. Analysis of DNA copy number identified focal deletion spanning the phosphatase and tensin homolog gene (*PTEN*; chr10, 89.53–89.62 MB) as a homozygous event in the original tumor and in both PDGFB and EGF-grown lines (Fig. S7*A*). This focal event is uncommon in GBM and unlikely to spontaneously occur twice.

Somatic mutation candidates from exome capture sequencing of the original tumor and derived lines were compared, and 53 candidate somatic mutations were identified from high-coverage regions (Fig. S7*B* and Table S1). There were three shared mutations equally present in each cell line at >90% allelic frequency. These three mutations were present in the original tumor at 52–81% frequency and were absent in blood at >100× coverage (101–356 reads). The remaining 50 candidate events appeared heterozygous. Of these, only one mutation, *MIER3* N532S, showed a significant skew in allelic frequencies of 58% and 20% in PDGFB and EGF populations, respectively ($P < 0.05$, Fisher exact test with Bonferroni correction). Therefore, although these candidate mutations have not been individually verified as somatic, all but one plausibly somatic mutation seemed to be shared by the majority of tumor cells in M753, and there is no evidence that the *EGFR*-amplified or *PDGFRA*/*EGFR* coamplified cells represent distinct clades.

Genetically Divergent Populations Can Emerge from Coamplified Parental Cells Without Specific Selection Through Unequal Segregation of Unstable Amplicons. Although selection of genotype can be induced by altering in vitro conditions, this should not be construed as evidence that similar mechanisms mediate the emergence of single-RTK genotypes in coamplified tumors during human tumor evolution. We investigated whether a simple model of cell replication with independent unstable amplicons could qualitatively reproduce the observed pattern without invoking any selection advantage for particular genotypes. Applying a simple model of binomial segregation as shown in Fig. 4, parental cells that harbor two independently amplified loci give rise to a tree of daughter cells, among which the majority show single RTK amplification or no amplification. Maintenance of coamplification in the same cell is statistically unlikely under the assumption of random segregation, and therefore coamplified cells constitute a minor population. The balance of genotypes in such a model is sensitive to DNA duplication rates of the independent loci and is readily modified by introducing selection (e.g., increased fitness for amplified or coamplified cells). However, within a wide range of model parameters for locus replication and selection, we found coamplified daughter cells to constitute the minor population when coamplified parental cells were expanded up to 10 logs (≈20 generations) (Fig. S8 *A*–*D*). The results of this simple model do not exclude the action of selection for genotype in the actual tumor. In fact, a degree of active selection for coamplification in the same cell is supported by the FISH results: coamplified cells are nearly always found in *EGFR*/*PDGFRA* coamplified tumors and therefore likely represent a common initiating event (i.e., a driver event). Rather, the model results establish that the range of genotypes seen in human tumors and the relative paucity of coamplified cells does not necessarily require active selection for single-RTK genotype and that selection mechanisms cannot be inferred from the FISH data alone.

Unequal segregation also provides a parsimonious explanation for the commonly observed pattern of *PDGFRA*-amplified cells interspersed with *EGFR*-amplified and coamplified cells: granular heterogeneity of genotype emerges from local lineage expansions. This does not exclude the possibility of more complex mechanisms as well; only that they are not required to explain the observed pattern. Cell–cell interactions between subpopulations, for instance, might improve fitness of the heterogeneous population compared with a clonal expansion. Such synergistic growth has been recently described between glioma cells expressing EGFRvIII and those expressing wild-type EGFR mediated by paracrine release of cytokines such as interleukin 6 and leukemia inhibitory factor (19). We investigated whether *EGFR*-amplified and *PDGFRA*-amplified cells might interact when cocultured in neurosphere conditions to manifest synergistic growth. The TS753 line enriched for PDGFRA amplification and protein expression by passage in PDGFB/gefitinib was admixed with the line similarly selected for EGFR by passage in EGF/imatinib (described in Figs. S4 and S5). Compared with the individual lines, admixtures of 1:1 or 3:1 (approximating the observed ratio in the parental tumor) demonstrated no synergistic growth under any of four conditions: with and without EGF, PDGF, or both ligands (Fig. S8*E*).

We compared drug sensitivities between the TS753 parental line and subpopulations selected under PDGFB/gefitinib and EGF/imatinib conditions. Results of two experiments are summarized in Fig. S9. In the first experiment, cells were incubated in PDGFB+EGF ligand. All three lines were treated with imatinib, gefitinib, or the PI3 kinase inhibitor LY294002 in a range of drug concentrations. Growth was assessed by resazurin viability assay at 0 and 6 d. In the second experiment, imatinib and gefitinib were tested singly and in combination while maintaining the cultures in their respective selection media (EGF or PDGFB only). Both experiments revealed a greater sensitivity to EGFR inhibition in the parental line (a mix of 100% *EGFR* amplified and 25–40% *PDGFRA* coamplified) than in either of the selected lines. Simultaneous treatment with both inhibitors seemed to have an additive effect in both of the selected lines.

Discussion

Gene amplification is the most common mechanism by which RTKs are altered in GBM (1, 3). These high-level amplifications usually comprise extrachromosomal double minutes, which are numerically unstable in proliferating populations owing to unequal mitotic segregation between daughter cells and/or variable replication (20–23). The maintenance of high copy number amplification throughout a population of cells is thought to

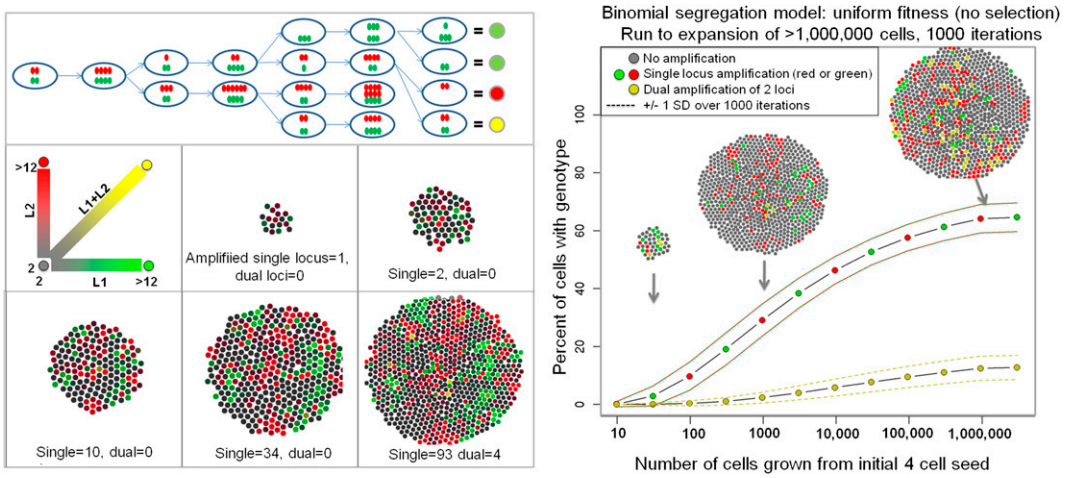

Fig. 4. Simulation results for the replication of cells harboring two independent unstable amplicons with uniform fitness (no selection advantage for gain of either locus). The simulation is initiated with four cells, each harboring two copies of locus L1 (green) and two copies of locus L2 (red). Cells divide randomly with probability of 0.5 per simulation step. With each cell division, the loci are replicated 2 times and randomly apportioned to the daughter cells, simulating the binomial segregation of unstable amplicons. *Left*: A single simulation of tumor expansion to 767 cells demonstrates enrichment for single-locus amplification and paucity of dual-amplified cells. *Right*: One thousand iterations run to >1,000,000 cells show convergence to a stable phenotype of ≈60% single-locus and 8% dual-locus amplified (amplification defined as eight or more copies). The pattern of granular heterogeneity and relative paucity of dual-amplified cells is qualitatively similar across a broad range of model parameters and does not require selective growth advantage conferred by the amplified loci (Fig. S8).

require continuous positive selection, and indeed loss of EGFR amplification in glioma cells is a common phenomenon with repeated in vitro passage (13, 24, 25). For the most commonly altered RTKs, EGFR and PDGFRA, amplification is associated with gene rearrangements that produce constitutively active receptor forms often expressed together with wild-type alleles (16, 19, 26). Unequal segregation of amplified alleles and regionally variable selection pressure provide one mechanism to explain the intratumoral heterogeneity of RTK copy number and expression of mutant forms seen in GBM (19, 27, 28).

Within this framework, there are several scenarios by which tumor cell subpopulations harboring independent RTK genotypes could emerge. In the simplest case, independent amplifications would arise by chance among a common parental tumor cell population or through polyclonal tumorigenesis. Polyclonal tumorigenesis was demonstrated in a recent study in which high-grade gliomas generated from a transgenic mouse model of Nestin-targeted PDGF expression were transplanted to nontransgenic animals (29). The implants were found to transform parenchymal cells in the recipient, forming tumors composed of tumor cells from both host and transplanted lineages. The pattern of clonal vs. subclonal mutations in a tumor can distinguish between these possibilities and define phylogenetic relationships between subpopulations (30–33). Both sequencing and CNA data from M753 and its derived lines support a model of late segregation of EGFR and PDGFRA genotypes in this tumor. This is concordant with analyses that suggest *EGFR* amplification is a late event in primary GBM tumorigenesis (the timing of *PDGFRA* amplification is unknown) (34). The finding that nearly all tumors in our study showed a significant subpopulation of cells harboring both *PDGFRA* and *EGFR* amplification suggests that both amplification events initially occur within a common parental cell, although fusion of tumor cells or DNA-containing exosomes is also plausible (35, 36).

The emergence of multiple single-RTK genotypes during GBM evolution likely represents an interaction between the unique genetics of unstable amplification and variable selection pressure related to tumor cell environment. We observed no large-scale structure in the distribution of *PDGFRA*-amplified cell populations among the coamplified cases studied here. Indeed, it is notable that *EGFR*- and *PDGFRA*-amplified cells could be found on FFPE sections from all cases selected by TCGA data derived from separate frozen tumor portions. *PDGFRA*-amplified cells were always found as a minor population and typically interspersed within fields of *EGFR*-amplified cells. This pattern may be accounted for by unequal segregation in cases of unstable amplification but could equally be explained by microenvironmental niches, cell–cell interactions, or even cell migration. The mechanisms by which independent RTK-amplified subpopulations arise and are selected for in vivo remain an open question and may be complex.

Although RTK coamplification seems to be present in at least 5% of TCGA samples overall, the prevalence is more significant when one considers the subset of GBM for which RTK amplification might be considered to signify a therapeutic target. We found that at least 14% of *EGFR*-amplified samples, 19% of *MET*-amplified cases, and 43% of *PDGFRA*-amplified cases have evidence of RTK coamplification by aCGH. The prevalence of coamplification is of significant importance for clinical trials of RTK inhibitor monotherapy in GBM, particularly those targeting PDGFR (37). It is also a consideration for inhibition of downstream pathway targets as well, because these subpopulations may exhibit different levels of downstream target activation and corresponding inhibitor sensitivities.

The phenomenon of GBM tumor cell subpopulations with distinct RTK activation may be more common than predicted by RTK coamplification alone. We previously reported that ≈30% of GBM demonstrate a pattern of PDGF-pathway activation at the protein level, even in the absence of *PDGFRA* amplification, and that this pattern could be found in *EGFR*-amplified and *MET*-amplified tumors (12). This finding is concordant with previous studies showing that PDGFRA protein is expressed in 25–30% of GBM, more often than the gene is amplified (38–40), and that PDGFR phosphorylation is commonly found in tumors with EGFR phosphorylation (11). It remains to be seen to what degree the finding of PDGFRA activation in *EGFR*- or *MET*-amplified GBM may define PDGF-supported subpopulations within these tumors. The genetic evidence provided in the present study suggests only a lower bound for tumors harboring such subpopulations.

In summary, this study takes advantage of the unique propensity for GBM to amplify RTKs to establish genetic evidence that multiple RTKs are likely maintaining distinct cell subpopulations. When present, these subpopulations each comprise significant fractions of the tumor and could plausibly contribute to the pattern of poor initial responses to RTK inhibitor monotherapies seen in clinical trials to date. It has been suggested that combination of two or more pathway inhibitors might be necessary to effectively treat GBM, but combining toxicities is a concern for safety and a limit to therapeutic dosing. We found that the majority of cells in coamplified tumors seem to harbor amplification of only one RTK, suggesting that unequal amplicon segregation and/or selection favor differentiation of genotype. If RTK dependence is similarly differentiated in a majority of cells, a trial of alternating therapy that avoids concurrent toxicity is a rational consideration.

Methods

TCGA Data Analysis. Array-CGH level 2 and level 3 datasets were downloaded from the public TCGA portal (Agilent CGH 244K platform, MSKCC source site) (3). Log2 ratios for *EGFR*, *PDGFRA*, and *MET* were determined from segmented (level 3) data by the maximum segment value across the gene. CNA focality was determined by GTS as previously described (15). Additional details in *SI Methods*.

Human Tumor Collection and Tumor Sphere Culture. Fresh human GBM tissue samples were obtained from patients who consented before surgery under an institutional review board-approved protocol. After deidentification, these tissue samples were banked as frozen tissue and used to generate tumor sphere cultures (*SI Methods*).

Tumor Sphere Preparation. Tumor specimen samples were washed in cold PBS twice, then manually dissociated and placed in Accumax (Innovative Cell Technologies) for 15 min under sterile conditions. Cells were subsequently washed and filtered through a 100-μm strainer and plated in NeuroCult NS-A proliferation media (Stemcell Technologies) supplemented with 10 ng/mL rhbFGF for all experimental conditions in the study. Initial cultures were also supplemented with 20 ng/mL rhEGF. Cells were incubated at normal oxygen levels at a temperature 37.0 °C and 5% CO_2. Additional details in *SI Methods*.

Inhibitor Treatments and Immunoblotting. Tumor sphere lines were grown in stem cell medium without growth factors for 18 h, followed by 4-h incubations with 4 μM gefitinib, 10 μM imatinib, or both. A negative control was incubated with an equivalent amount of DMSO. After drug incubations, cells were activated with 100 ng/mL EFG and/or 100 ng/mL PDGFB as indicated. Incubations in presence of ligand were left for 20 min before harvesting the cells. Immunoblotting, antibodies, and growth assay methodology are described in *SI Methods*.

Flow Cytometry and Sorting. TS753 cells were growth factor starved overnight. Cells were preincubated in 1:20 dilution of Fc block (Biolegend, #422301) in 1% BSA/PBS for 30 min at room temperature. Cells were either fixed and permeabilized (Fig. S5*A*) or not (Fig. S5*B*) before FACS (additional details in *SI Methods*).

Simulation of Binomial Segregation. Simulations were performed in R (http://cran.r-project.org). Each simulation run begins with an initial seed of four cells, each assigned equal copies of both loci. For simulations with uniform fitness (no selection), seed cells are initialized with two copies of each locus; for models with selection, 25 copies of each locus are used. Replication cycles are then simulated. The probabilities for selection models and additional details are given in *SI Methods*.

ACKNOWLEDGMENTS. We thank Agnes Viale and Maryam Hassimi for assistance in sequencing. This work was supported by the Leon Levy Foundation (N.J.S. and C.W.B., Leon Levy Scholar), National Institutes of Health Grant P01-CA95616 (to C.W.B.), and The Brain Tumor Center at Memorial Sloan-Kettering Cancer Center.

1. Furnari FB, et al. (2007) Malignant astrocytic glioma: Genetics, biology, and paths to treatment. *Genes Dev* 21:2683–2710.
2. Bondy ML, et al.; Brain Tumor Epidemiology Consortium (2008) Brain tumor epidemiology: Consensus from the Brain Tumor Epidemiology Consortium. *Cancer* 113(7, Suppl)1953–1968.
3. Cancer Genome Atlas Research Network (2008) Comprehensive genomic characterization defines human glioblastoma genes and core pathways. *Nature* 455: 1061–1068.
4. Huse JT, Holland EC (2010) Targeting brain cancer: Advances in the molecular pathology of malignant glioma and medulloblastoma. *Nat Rev Cancer* 10:319–331.
5. De Witt Hamer PC (2010) Small molecule kinase inhibitors in glioblastoma: A systematic review of clinical studies. *Neuro Oncol* 12:304–316.
6. Krishnan S, et al.; North Central Cancer Treatment Group (2006) Phase I trial of erlotinib with radiation therapy in patients with glioblastoma multiforme: Results of North Central Cancer Treatment Group protocol N0177. *Int J Radiat Oncol Biol Phys* 65:1192–1199.
7. Paulsson J, et al. (2011) Prognostic but not predictive role of platelet-derived growth factor receptors in patients with recurrent glioblastoma. *Int J Cancer* 128:1981–1988.
8. Hasselbalch B, et al. (2010) Prospective evaluation of angiogenic, hypoxic and EGFR-related biomarkers in recurrent glioblastoma multiforme treated with cetuximab, bevacizumab and irinotecan. *APMIS* 118:585–594.
9. Hegi ME, et al. (2011) Pathway analysis of glioblastoma tissue after preoperative treatment with the EGFR tyrosine kinase inhibitor gefitinib—a phase II trial. *Mol Cancer Ther* 10:1102–1112.
10. Raizer JJ, et al.; North American Brain Tumor Consortium (2010) A phase II trial of erlotinib in patients with recurrent malignant gliomas and nonprogressive glioblastoma multiforme postradiation therapy. *Neuro Oncol* 12:95–103.
11. Stommel JM, et al. (2007) Coactivation of receptor tyrosine kinases affects the response of tumor cells to targeted therapies. *Science* 318:287–290.
12. Brennan C, et al. (2009) Glioblastoma subclasses can be defined by activity among signal transduction pathways and associated genomic alterations. *PLoS ONE* 4:e7752.
13. Okada Y, et al. (2003) Selection pressures of TP53 mutation and microenvironmental location influence epidermal growth factor receptor gene amplification in human glioblastomas. *Cancer Res* 63:413–416.
14. Giannini C, et al. (2005) Patient tumor EGFR and PDGFRA gene amplifications retained in an invasive intracranial xenograft model of glioblastoma multiforme. *Neuro Oncol* 7:164–176.
15. Wiedemeyer R, et al. (2008) Feedback circuit among INK4 tumor suppressors constrains human glioblastoma development. *Cancer Cell* 13:355–364.
16. Ozawa T, et al. (2010) PDGFRA gene rearrangements are frequent genetic events in PDGFRA-amplified glioblastomas. *Genes Dev* 24:2205–2218.
17. Verhaak RG, et al.; Cancer Genome Atlas Research Network (2010) Integrated genomic analysis identifies clinically relevant subtypes of glioblastoma characterized by abnormalities in PDGFRA, IDH1, EGFR, and NF1. *Cancer Cell* 17:98–110.
18. Liu KW, et al. (2011) SHP-2/PTPN11 mediates gliomagenesis driven by PDGFRA and INK4A/ARF aberrations in mice and humans. *J Clin Invest* 121:905–917.
19. Inda MM, et al. (2010) Tumor heterogeneity is an active process maintained by a mutant EGFR-induced cytokine circuit in glioblastoma. *Genes Dev* 24:1731–1745.
20. Bigner SH, Vogelstein B (1990) Cytogenetics and molecular genetics of malignant gliomas and medulloblastoma. *Brain Pathol* 1:12–18.
21. Thiel G, et al. (1992) Karyotypes in 90 human gliomas. *Cancer Genet Cytogenet* 58: 109–120.
22. Lopez-Gines C, et al. (2010) New pattern of EGFR amplification in glioblastoma and the relationship of gene copy number with gene expression profile. *Mod Pathol* 23:856–865.
23. Kimmel M, Axelrod DE (1990) Mathematical models of gene amplification with applications to cellular drug resistance and tumorigenicity. *Genetics* 125:633–644.
24. Bigner SH, et al. (1990) Characterization of the epidermal growth factor receptor in human glioma cell lines and xenografts. *Cancer Res* 50:8017–8022.
25. Fael Al-Mayhani TM, et al. (2009) An efficient method for derivation and propagation of glioblastoma cell lines that conserves the molecular profile of their original tumours. *J Neurosci Methods* 176:192–199.
26. Nishikawa R, et al. (1994) A mutant epidermal growth factor receptor common in human glioma confers enhanced tumorigenicity. *Proc Natl Acad Sci USA* 91:7727–7731.
27. Pandita A, Aldape KD, Zadeh G, Guha A, James CD (2004) Contrasting in vivo and in vitro fates of glioblastoma cell subpopulations with amplified EGFR. *Genes Chromosomes Cancer* 39:29–36.
28. Witusik-Perkowska M, et al. (2011) Glioblastoma-derived spheroid cultures as an experimental model for analysis of EGFR anomalies. *J Neurooncol* 102:395–407.
29. Fomchenko EI, et al. (2011) Recruited cells can become transformed and overtake PDGF-induced murine gliomas in vivo during tumor progression. *PLoS ONE* 6:e20605.
30. Navin N, et al. (2010) Inferring tumor progression from genomic heterogeneity. *Genome Res* 20:68–80.
31. Navin N, et al. (2011) Tumour evolution inferred by single-cell sequencing. *Nature* 472:90–94.
32. Stephens PJ, et al. (2011) Massive genomic rearrangement acquired in a single catastrophic event during cancer development. *Cell* 144:27–40.
33. Campbell PJ, et al. (2008) Subclonal phylogenetic structures in cancer revealed by ultra-deep sequencing. *Proc Natl Acad Sci USA* 105:13081–13086.
34. Attolini CS, et al. (2010) A mathematical framework to determine the temporal sequence of somatic genetic events in cancer. *Proc Natl Acad Sci USA* 107:17604–17609.
35. van der Vos KE, Balaj L, Skog J, Breakefield XO (2011) Brain tumor microvesicles: Insights into intercellular communication in the nervous system. *Cell Mol Neurobiol* 31:949–959.
36. Balaj L, et al. (2011) Tumour microvesicles contain retrotransposon elements and amplified oncogene sequences. *Nat Commun* 2:180.
37. Raymond E, et al.; European Organisation for Research and Treatment of Cancer Brain Tumor Group Study (2008) Phase II study of imatinib in patients with recurrent gliomas of various histologies: A European Organisation for Research and Treatment of Cancer Brain Tumor Group Study. *J Clin Oncol* 26:4659–4665.
38. van der Valk P, Lindeman J, Kamphorst W (1997) Growth factor profiles of human gliomas. Do non-tumour cells contribute to tumour growth in glioma? *Ann Oncol* 8:1023–1029.
39. Haberler C, et al. (2006) Immunohistochemical analysis of platelet-derived growth factor receptor-alpha, -beta, c-kit, c-abl, and arg proteins in glioblastoma: Possible implications for patient selection for imatinib mesylate therapy. *J Neurooncol* 76:105–109.
40. Martinho O, et al. (2009) Expression, mutation and copy number analysis of platelet-derived growth factor receptor A (PDGFRA) and its ligand PDGFA in gliomas. *Br J Cancer* 101:973–982.